INDIVIDUAL DELINEATION OF OIL PALM TREE USING WORLDVIEW02 SATELLITE IMAGE

Alexius KOROM[a], Mui-How PHUA[b], Yasumasa HIRATA[c] and Toishiya MATSUURA[c]

[a]Universiti Teknologi MARA (UiTM) Cawangan Sabah,
Beg Berkunci 71, 88997 Kota Kinabalu, Sabah, Malaysia;
E-mail: alexi502@sabah.uitm.edu.my

[b]School of International Tropical Forestry, Universiti Malaysia Sabah (UMS),
Locked Bag No. 2073, 88999 Kota Kinabalu, Sabah, Malaysia;
E-mail: pmh@ums.edu.my

[c]Forestry and Forest Products Research Institute,
Matsunosato 1, Tsukuba, Ibaraki, 305-8687, Japan;
E-mail: hirat09@affrc.go.jp, matsuu50@affrc.go.jp

KEY WORDS: Individual delineation, oil palm, pixel-based masking, object-based segmentation, segmentation goodness measures

Abstract. Individual extraction of single tree remained as a challenging process in remote sensing using high resolution multispectral images. In this paper, a combination of pixel-based masking and object-based segmentation has been successfully presented for the individual delineation of oil palm (*Elaeis guineensis*) tree. The study site area is situated at FELCRA Berhad Estate Sungai Ruku-Ruku in the Beluran district of Sabah (North Borneo). A total of sixteen plots were surveyed based on strata random pattern within the 166 hectares area of an old oil palm plantation aged between 24 to 25 years. Every plot has a radius of 15 meter which consists of approximately eight to thirteen trees inside it. In the analysis, relative position of each surveyed trees taken using a moderately accurate handheld GPS has been spatially corrected. Three pansharpened multispectral bands were regularly used in this approach that were the red, red edge and also near infrared. Further manipulations were carried out using the vegetation indices such as the normalized difference vegetation index (NDVI), normalized difference infrared index (NDII) and differential vegetation index (DVI) as a masking filter layer. Finally, the segmentation process was then carried out using the watershed technique before it was assessed using the modified Moller's area and location based for segmentation goodness measures. Parameter setting analysis was also provided to search out the best threshold values used to segment each individual tree. Result from the analysis shows a good segmentation rate up to 100% percent from the total evaluated trees that were successfully segmented. On the other hand, the oversegmentation and undersegmentation coefficient calculated for the segmentation product were 0.3161 and 0.1882 respectively approaching the zero value for perfect shape matching condition. In terms of centroid gap distance, the value of goodness measure is 0.4010. Lastly, the global performance was evaluated as 0.3142.

1. INTRODUCTION

Geographic Object-Based Image Analysis (GEOBIA) approach in analyzing the high resolution images are evolving faster in recent years. (Blaschke 2010, Hay and Blaschke 2010, Addink, Van Coillie et al. 2012) cover vast research area such as urban structure identification (Agüera and Liu 2009), landslide risk evaluation (Aksoy and Ercanoglu 2012), landscape identification (Akbari, Shea Rose et al. 2003), coastal zone management (Fornes, Basterretxea et al. 2006, Krause, Bock et al. 2010), health monitoring (Addink, De Jong et al. 2010), riparian vegetation mapping (Akasheh, Neale et al. 2008), rainfall estimation (Anagnostou, Kalogiros et al. 2010), for military purposes (Chang, Eo et al. 2011), Lidar individual tree delineation (Kwak, Lee et al. 2007, Wang, Birt et al. 2011), forest canopy gap estimation (Zhang 2008, Hu, Gong et al. 2009) and tree species identification (Koukoulas and Blackburn 2005, Leckie, Gougeon et al. 2005, Bunting, He et al. 2009). Along the path of GEOBIA chronologies, it has shown that technology enhancement, satellite improvement, sensor refinement as well as the availability of commercial software and the success of previous conferences have all contributed to the field (Blaschke 2010, Addink, Van Coillie et al. 2012). Nowadays, the GEOBIA research development is still evolving to find a better way

towards the further exploration of a high resolution data.

Previously, a pixel-based classification was often used to classify feature objects on the images. In environmental studies, it is very useful to extract information based on the spectral signature of the corresponding object on earth (Foody, Boyd et al. 2003, Thenkabail, Stucky et al. 2004, Morel, Fisher et al. 2012). Throughout the remote sensing development more advance analysis, the object-based classification, is able to detect additional information such as the size, shape, texture and also nearby object occurrences related to the other. Obviously, object-based approaches have an advantage over the pixel-based in terms of object recognition where spatial information was able to be used as medium of interpretation. Back to basic, it is all about interpreting a segment polygon that is extracted from the images. Perceptibly, behind all the efforts, the object segmentation is the primary base work.

In this paper, we studied the best usage of vegetation indices to improve the segmentation algorithm for individual tree using a submeter resolution Worldview02 multispectral satellite data. The subject of interest in this paper is the oil palm or its scientific name is *Elaeis guineensis*. A semi-automatic segmentation algorithm had been applied unto the satellite image which was divided into two main parts; the image filtering process and object-based segmentations. The aim of object-based segmentation part is to delineate every single unit of tree inside the oil palm plantations. Afterwards, an accuracy assessment was then carried out unto each successfully segmented oil palm trees with regards to their respective collected ground plot data. The results are presented and discussed in detail in the following pages.

2. STUDY AREA

The study site is situated in the district of Beluran at about 120 km to the west of Sandakan city, the second largest town in Sabah (North Borneo), Malaysia. Three blocks (A8, A9 and A10) covering an area of 166 hectares located at FELCRA Berhad Estate Sungai Ruku-Ruku, Beluran had been chosen for ground plot data collections as shown in Figure 1. The surrounding is an undulating terrain with an elevation ranging from 60 to 138 meter from sea mean level. The Ruku-Ruku river crossed right through the middle of the site flowing from South heading to the West which provides the estate enough quantities of water supply to irrigate the palms during the dry season in May-September. The river also helps to flow out excess water runoff during the rainy season in November-March. The whole estate has been in operation since the year 1985 operated by its two former owners, Sri Ranau Sdn Bhd and Ladang Sugut Sdn Bhd, before it was sold to a government link company, the Federal Land Consolidation and Rehabilitation Authority or FELCRA in year 2000. Most of the oil palms in this estate are in their matured phase and now replanting is ongoing to replace the old and over matured trees. During the data collection period, about 20% of the area was cleared up for the transplanting of new young palms.

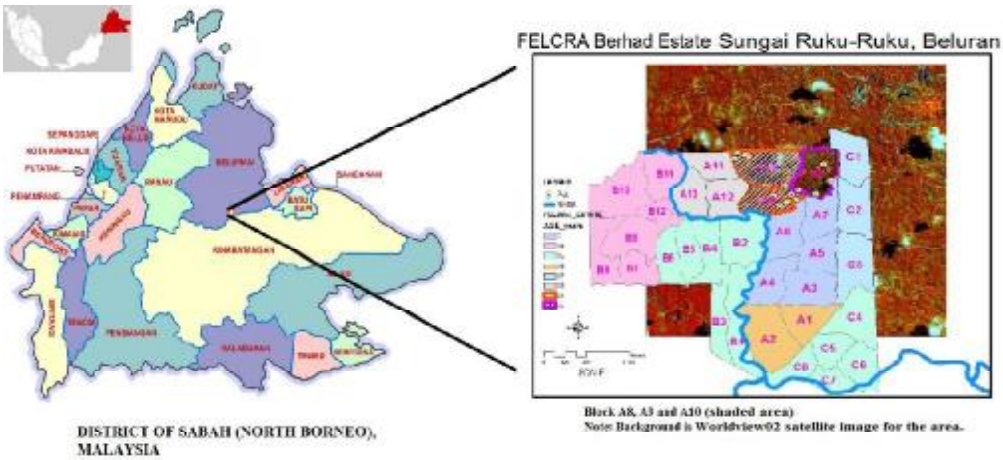

Figure 1: Study site

Worldview02 satellite image

Image was obtained from Worldview02 satellite which was captured on May 10, 2010 over an extending area from top (612310) to bottom (607188) and left (530143) to right (535157) according to map datum Universal Transverse Mercator (UTM) Zone 50N. This image has been radiometrically corrected and geometrically orthorectified using DEM data of SRTM 30 meter before hands over to the customer. However, about 10% from the total area of whole image was covered by the clouds.
Worldview02 consist two types of high resolution data images that are panchromatic and multispectral. Each of these data layers has a resample spatial resolution of 0.5 meter and 2 meter respectively. Based on the present spatial resolution of colour multispectral data, it is insufficient to detect the tree object efficiently. A better result in object identification was obtained after the fusion of the multispectral data with finer panchromatic image layer (Ardila, Tolpekin et al. 2011). Same approach has been applied unto the Worldview02 data image in this study.

DATA COLLECTION

Data was collected from sixteen (16) plots in stratify random way. Each plot is a circular shape with a radius of 15 meter consisting of eight to thirteen trees inside it. All the confined trees are going to be used to verify the existence and location of a successfully segmented tree object later on. The locations of all these trees were relatively calculated based on the GPS midpoint of the plot. An average time around 20 minutes was spent to take a GPS reading of the plot's midpoint.

GPS data corrections

Correction must be done before the GPS data can be utilized to verify each respected segment. A pair matching identification technique has been applied here to find connectivity between the uncorrected GPS tree point and manually detected tree. The plot's midpoint location was previously taken using the handheld GPS Garmin which possesses accuracy about ±10 meter thus there is a tendency that the GPS reading can deviate from its true location. The reading needs to be corrected accordingly before being used in the segment verification process. Here, two guidance criterions were used to perform the correction that are the nearest position and distributed pattern of each highlighted tree. Connectivity between the uncorrected GPS tree point and the manual detected tree was explored this way as illustrated in Figure 2.

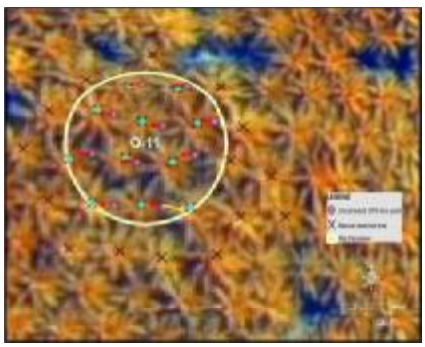

Figure 2: Pair matching identification of GPS point

The distribution patterns of trees inside the plot were easily understood using ArcGIS query function. A circular plot's line drawn in the figure, which enclosed around eight to thirteen trees, was averagely shifted a little bit after the deviated distance and direction was determined. The layer of manually detected trees was used to steer in the process of tracking back the GPS deviation's distance and direction by applying a buffer at increase interval using the function of *select-by-location*. It was found out from the process that error associated with the GPS data point is ranging from 2.5 to 9 meter with mostly the error have occurred at the centre of 5 meter from the overall accuracy limit of ±10 meter. Additionally, this direction error can also be determined based on the most similar pairs pattern between uncorrected GPS tree point and highlighted manual tree point, as in the above Figure 2 it is heading west (red colour arrow) about 3 to 5m distance and not to the east (yellow colour arrow) direction.

3. INDIVIDUAL DETECTION ALGORITHM

The crown component of oil palm images appear to be scattered rather than forming a nicely bounded crown due to its pinnate-leaved stand structure which is a bit lower at the columnar stem centre compare to the surrounding crown perimeter ((FAO) 1970). Morphologically, looking on the image, this crown shape has created a dark-bright fluctuation like salt and pepper appearances that make it difficult to build a single segment to represent a single object. Previously, the object-based analysis on oil palm was classified only at the general level rather than individual object (Morel, Saatchi et al. 2011, Santoso, Gunawan et al. 2011).

Some object classification works were based on the idea of manipulating a spectral band for vegetation indices (Peña-Barragán, Ngugi et al. 2011, Santoso, Gunawan et al. 2011). Our studies also have similarities with their work where certain bands were manipulated as vegetation index for better visualization and interpretation. These layers were then used in smart algorithm to recognize the pattern of oil palm object as intelligently as human interpret it (Tansey, Chambers et al. 2009, Santoso, Gunawan et al. 2011). Therefore, in this paper, three basic steps were brought up in dealing with a multispectral dataset that are: a) image preprocessing, b) image segmentation, and c) segmentation assessment (Korom and Phua 2011).

Worldview02 dataset consists of eight bands namely coastal (C: 400-450nm), blue (B: 450-510nm), green (G: 510-580nm), yellow (Y: 585-625nm), red (R: 630-690nm), red edge (RE: 705-745nm), near infrared 1 (NIR1: 770-895nm) and near infrared 2 (NIR2: 860-1040nm). Each band combinations are very useful to study on particular applications such as bathymetry, vegetation health and biomass studies. However, in these study only three bands, the red, red edge and near infrared were used in the algorithm development phase. These are the bands that are useful to generate vegetation indices such as NDVI, NDII and DVI. The formula for each index is stated in Table 1 as follows:

Table 1: Vegetation indices (equation; copied and modified from (Gonsamo and Pellikka 2012))

Vegetation Index (VI)	Formula	Value range	Reference
Normalized Difference Vegetation Index (NDVI)	$NDVI = \frac{NIR - R}{NIR + R}$	-1 to +1	(Rouse, Haas et al. 1974)
Normalized Difference Infrared Index (NDII)	$NDII = \frac{NIR - RE}{NIR + RE}$	-1 to +1	(Hardisky, Klemas et al. 1983)
Differential Vegetation Index (DVI)	$DVI = NIR - R$	∞	(Richardson and Everitt 1992)

Pixel-based masking

Under this procedure, one layer mask is needed to filter the unwanted pixels which belong to other object other than the oil palm. Thus it enables the next procedure just to concentrate only on individual segmentation of the oil palm tree. In order to do so, there are two phases of task involved in the algorithm procedure which is manipulating the vegetation index as a filter layer. Firstly, three types of land object which were categorised as the barren surface, vegetations and other object such as metal and rock mineral. Here, a technique of boosting up the DVI layer by multiplying it with (NDVI + 1) layer was introduced at the early step. The major impact of this technique is that it has brought down the brightness of pixel value at places which have low quantities of vegetation and yet, has boosted up those pixels with high quantities of vegetation. Such an effect enables a fine parameter setting for the determination of more accurate threshold value to separate between the three on-land objects based on its pixel brightness criteria. This process we referred to as Threshold Filter 1 (TH1) parameter setting as summarized in Table 2.

The next task is dealing with the further sub classification of the vegetation class. Here, the oil palm was separated from other types of vegetation such as the shrubs, grasses and different tree species with the helps from NDII layer as filter. And again, the threshold lower and upper limit values were strategically determined which we referred to as Threshold Filter 2 (TH2) parameter setting. Through this way we managed to differentiate each pixel whether it belong to the oil palm or shrubs and grasses. But one has to be extra careful during selection of the correct lower and upper limit of the threshold brightness value because there is no clear cut where the value can really clarify a transition between oil palm and the other

vegetation objects. Furthermore, the threshold value is very much subjected to the quality of satellite images which is affected by ground atmosphere-environment conditions and camera sensor efficiency during the time the data was captured. Thus, for high accuracy purposes, it is recommended to assess the local parameter setting whenever doing a segmentation project at a particular region which involves tedious work.

Table 2: Analysis range for threshold lower and upper limit value

Classification region:	Entire image	Class 2
Threshold filter:	TH1	TH2
Categories:	min > Class 1 > TH1low	min >= SubClass 1 > TH2low
	TH1low >= Class 2 >= TH1up	TH2low >= SubClass 2 > TH2up
	TH1up > Class 3 > max	TH2up >= SubClass 3 > max

In trying to get the best segmentation for each oil palm tree, we discovered one problem associated with the algorithm. For pixel-based masking, picking the unwanted pixels out of the entire data layer is a challenging process where it requires perfect definitions of threshold value setting. In fact we have to admit that it is very difficult to get a perfect setting for the threshold. It is a rare case when the isolated null pixel did occur within the object bodies caused by the imperfect filtering of the high resolution image but it does create such a problematic segmentation during the algorithm implementation.

Object-based segmentation

Our aim is to get a better segmentation for high resolution images based on single-object level rather than a multi-object level. And of course, in this paper, the idea behind of the overall effort is to reduce the complexity of image into a single-object level before performing the segmentation task. Through this approach, it is easier to focus on the single-object rather than trying to do segmentation for multi-object at one time. There are many types of segmentation methods that can be implemented to achieve the final objective of individual tree delineation such as the region growing, top-down contour, edge detection and watershed transformation.

In this case, watershed segmentation looks good for the task which was successfully proven when applied unto various applications such as forest tree individual identification, building rooftop delineation, road mapping and many more. In watershed transformations, the gradient magnitude of an image will be treated as a topographic surface where a high contrast of intensities corresponds to watershed lines or region boundaries. In doing so, the image will undergo processes: a) reverse a maximum to minimum value, and b) delineate the watershed lines after virtually pouring water on it. Through this method, water flows from uphill to downhill which refer to as the common local minimum point and act as an individual catchments basin.

IMAGE SEGMENTATION GOODNESS MEASURES

Moller (2007) has suggested an object metrics validation to assess the performance of image segmentation algorithm. Later it was then modified by Clinton (2010) which specifically developed an assessment procedure for object-based segmentation problem. Their method has been adapted in this paper to assess the individual delineated oil palm tree extracted from a submeter resolution images. Only a successfully matched pair between the manual digitized training object and auto developed segment objects was considered in this paper.

The success rate was calculated using below equation (1).

$$Successful\ segmentation\ rate, r_{suc} = \frac{Number\ of\ success\ segmentation}{Total\ of\ trees} \quad (1)$$

It was believed that the imperfect pixel masking is the reason behind why full capacities of segment generation cannot be achieved. Subsequently, the remaining trees are then evaluated accordingly based on their coincided area and centroid gap distance between the manual digitized training object and auto developed segment object. The technical explanations about the theories are provided on the next subsections.

Formula for area-based goodness measures

Let the polygons of manually digitized training object is represent by $A = \{a_i : i = 1,2 \dots n\}$ and the auto developed segment object is represent by $B = \{b_j : j = 1,2 \dots m\}$. Oversegmentation formula for each successfully matched pair ij between manual digitized training object and auto developed segment object is stated as below:

$$Oversegmentation, OSeg_{ij} = 1 - \frac{area(a_i \cap b_j)}{area(a_i)}, \; b_j \in B_i^* \tag{2}$$

where a_i = manual digitized training object,
b_j = auto developed segment object,
B_i^*= union of all possibilities matching cases, and
$area(a_i \cap b_j)$ = coincide area between a_i and b_j.

And the same happens to the undersegmentation case with formula below:

$$Undersegmentation, USeg_{ij} = 1 - \frac{area(a_i \cap b_j)}{area(b_j)}, \; b_j \in B_i^* \tag{3}$$

For both oversegmentation and undersegmentation cases, the scale range is (0, 1) where 0 represents perfect condition and vice versa. However, entire evaluations for the segments are crucial. So in global terms, the average sum of all matched pairs is stated as below:

$$Global\ oversegmentation, GOSeg = \sqrt{\frac{\sum_{l=1}^{k} OSeg_{ij,l}^2}{(k-1)}} \tag{4}$$

$$Global\ undersegmentation, GUSeg = \sqrt{\frac{\sum_{l=1}^{k} USeg_{ij,l}^2}{(k-1)}} \tag{5}$$

where k is the total number of matched pair between manually digitized training object and auto developed segment object.

Formula for location-based goodness measures

The gap distance between the centroid of training object and segment object was used to define a mismatch location between them. Let say, if centroid of a_i is (x_i, y_i) and centroid of b_j is (x_j, y_j) then their gap distance can be written as follow:

$$\left|dist_{a_i - b_j}\right| = \sqrt{(x_i - x_j)^2 + (y_i - y_j)^2} \tag{6}$$

If term $\left|dist_{a_i - b_j}\right|$ is simplified to $\left|dist_{ij}\right|$ then its relative position can be calculated using below formula:

$$Relative\ position, RP_{ij} = \frac{dist_{ij}}{dist_{ijMax}} \tag{7}$$

where $\left|dist_{ijMax}\right|$ is the largest gap distance from the total matched pair. Thus, similar case with area-based goodness measures then the overall segment's location-based evaluation was calculated based on formula below.

$$Global\ gap\ distance, GapD = \sqrt{\frac{\sum_{l=1}^{k} RP_{ij,l}^2}{(k-1)}} \tag{8}$$

The scale range for relative position is also (0, 1) with 0 reflects unto the most perfect cases and vice versa.

Formula for combined goodness measures

Finally, the area-based and location-based goodness measures were then combined to get the overall assessment for segmentation accuracy using formula below:

$$Combined\ segmentation\ goodness\ \ measures, CSGM = \sqrt{\frac{GOSeg^2 + GUSeg^2 + GapD^2}{3}} \tag{9}$$

Bear in mind, statistically, the equation 9 is an average of square root value of the global variance segmentation goodness measures.

4. RESULTS

Parameter Setting Analysis

There is no baseline on how and where to initiate a starting point for threshold lower and upper limit. But first, it is suggested at least to do some exploration on the pixels at the edge line of an object. A strategic iterative analysis was performed in this paper for both threshold filters, TH1 and TH2, in Table 2. After examined some object's edge line, below specifications was suggested for testing:
TH1: i=0 to 6; TH1low=50 to 650, Δ_{low}=100 and TH1: j=0 to 4; TH1up=600 to 1400, Δ_{up}=200
TH2: i=0 to 3; TH2low= -0.1 to 0.3, Δ_{low}= 0.1 and TH2: j=0 to 5; TH2up= 0.2 to 0.45, Δ_{up}= 0.05
Each Δ_{low} and Δ_{up} is the iteration interval for a lower and upper limit. Apply them into the newly developed algorithm then we managed to get some results which are presented below.

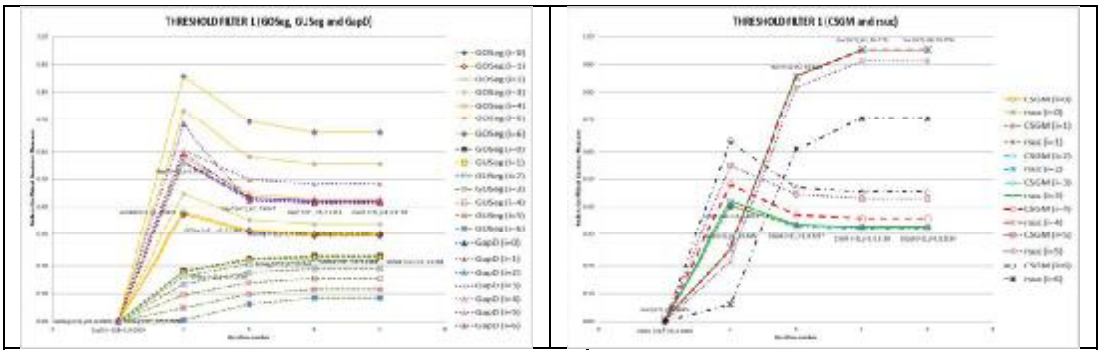

(a) **TH1 change | TH2 constant**

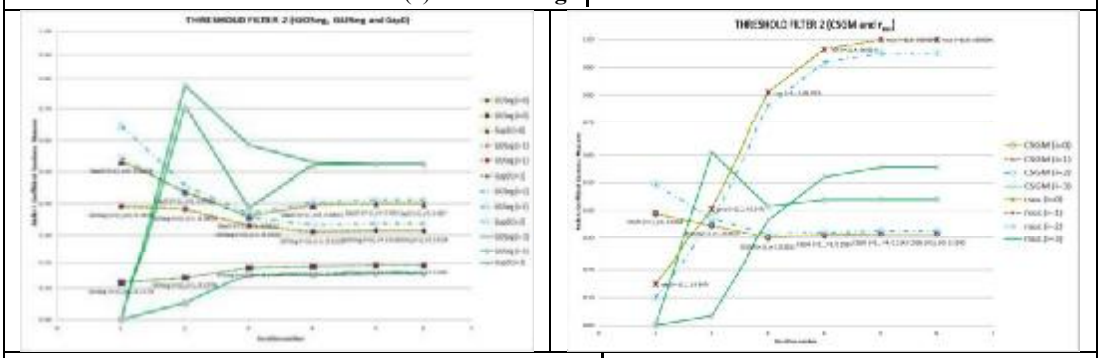

(b) **TH1 constant | TH2 change**

Figure 3: Graph performance of each succeeded iteration, i-th and j-th
X-axis: Iteration number; and Y-axis: Moller's coefficient

A total about 148 trees from sixteen plots of ground survey have been used in the evaluations. Success rate for segmentation was calculated based on the successfully matched pair between the extracted tree segment and GPS corrected tree. Each of polygon goodness measures were calculated using a previous mentioned equations and then the sum of all measures which resulted in global assessment are put in illustrative figure for better analysis.

Simple analysis by plotting a performance graph to envisage the calculated result can be seen in Figure 3. Two types of settings were analyzed by changing the threshold lower limit while putting the upper limit at constant to see the changes in their respective global performance and vice versa. It was then increased slowly based on preset interval value for each lower and upper limit level. The first filter, TH1, shows about four iterations were enough for the result to converge at 95.27% successful rate. Where else, for second filter, TH2, the fourth iteration give a reasonable converged result at around 96.62% but next iteration will result in 100% successful segmentation rate.

Segmentation Algorithm

In general, the final result of the overall task is the individual segment of each oil palm trees which extracted from the images. An intelligent but yet simple and easy to follow algorithm are tried to be developed which accurately and robustly perform the segmentation task using an input of submeter high resolution Worldview02 satellite images. It started with the three original multispectral bands and the image was then pan sharpened using the panchromatic layer with finer resolution at 0.5 meter to improve the image visuals. Next, vegetation indices were then formed and used to filter out the unwanted object classes such as the barren surface, metal or rock mineral and other vegetations (grasses, shrubs and bushes). The processes left only the oil palm object to remain in the final output image for input to watershed segmentation. Besides detecting the three land objects, the normalized difference vegetation index or NDVI also is very useful in separating the clouds and its ground shadow. The infrared vegetation index or NDII was then used in further detecting the small portions of grasses and shrubs. Therefore, the results of the major algorithm processes are shown in sequence at Table 3.

Table 3: Example of segmentation algorithm results

Step	Images	Explanations
1.	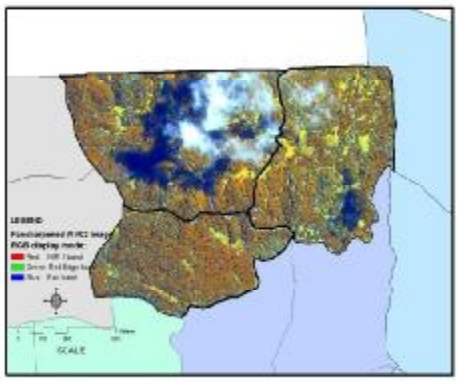	<u>RGB display mode: NIR 1, Red Edge and Red</u> A view of Worldview02's satellite image of Block A8, A9 and A10. This pansharpened image possesses a good visual for normal human eye detection of spatial stratum which was used for locating ground plots. A presence of about 30% coverage of cloud and its shadow will be discarded at the next filtering step.
2.	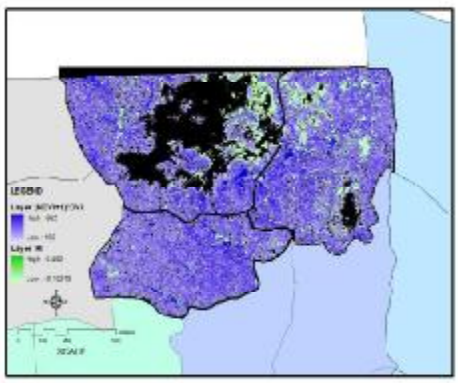	<u>Pixel-based Masking Process</u> **TH1**: Constant Filtered region: Black area Class 1: min to TH1low (discarded) Class 2: TH1low to TH1up (accepted) Class 3: TH1up to max (discarded) **TH2**: Change (i=1, j=4) Filtered region: Light green area Subclass 1: min to TH2low (discarded) Subclass 2: TH2low to TH2up (accepted) Subclass 3: TH2up to max (discarded)

3.	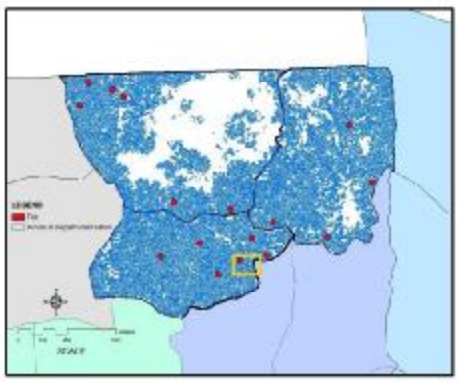	Individual Tree Segment Extraction r_{suc} = 100.00% GOSeg = 0.3161 GUSeg = 0.1882 GapD = 0.4010 CSGM = 0.3142 Focus area (yellow colour rectangle box) was presented in Figure 4 to larger illustration of the individual extraction's result.

Individual Delineation Results

Figure 4 is the enlarged result of the above algorithm which shows every individual oil palm trees are nicely delineated and represented by one polygon. We provide manual tree delineated segments, represented by pink colour irregular shape, as a comparison to show the difference of the segments from auto-generated one. Subjected upon a personal judgement, different person may digitize a tree differently. So it is good if a second opinion is gathered regarding the digitized layer before proceeding to the next evaluation step. Based on the above figure, the light blue line represents each individually auto-segmented oil palm tree. Notice that each segment is having a significant area and perimeter approaching the size and dimension of the manually digitized oil palm object. However, the segmentation procedure was not perfect and is still associated with some errors. It can be seen from the figure that some polygons at boundaries are quite small and does not represent a size of one mature or old palm tree (purple circle). And furthermore, some oil palm objects are shown divided into two or more polygons which should not be happened (yellow circle).

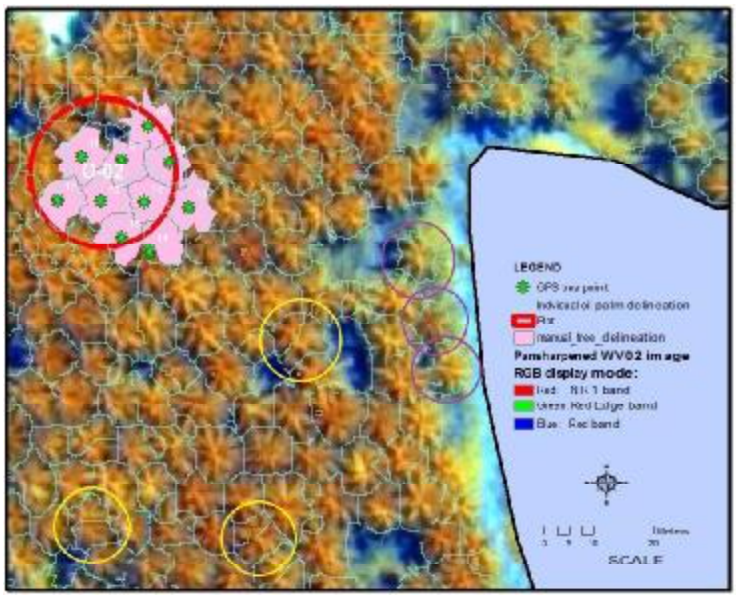

Figure 4: Individual delineation result

Generally, the assessment is about a shape comparison between the auto-generated segment and personal digitized segment. It is not about how accurate the segment is because a true shape of oil palm tree is not available. It is difficult to get a perfect true shape of oil palm from the satellite images. However, approximating true shape evaluation still can be applied unto the segments.

General comparison

Apparently, compare to a common tropical tree, the oil palm has a different crown shape and texture which makes it a little bit difficult to be segmented individually. Meanwhile, the crown of a coniferous tree is the easiest shape to be detected and segmented by using the multispectral images based on manipulation of the local maximum characteristics (Leckie, Gougeon et al. 2005). In standard practice, the peak of tree will be represented by a local highest brightness pixel and this can be easily detected using the water basin technique (Wulder, Niemann et al. 2000).

Here, a direct general comparison has been made between our newly developed segmentation algorithm and the standard RGB segmentation to investigate the difference between them. Usually, procedure for automatic individual segmentation using a normal RGB band is difficult due to the natural shape and morphological form of the oil palm tree as can be seen in Figure 5. Basically, the figure is about the same image but showing different results produced from two different algorithms using same ArcGIS software with segmentation watershed technique. The yellow line indicates an automatic segmentation and the pink line indicates a manually digitized palm tree inside one plot. We can conclude that the newly developed algorithm provides a quite good segmentation quality compare to over segmented result in Figure 5a.

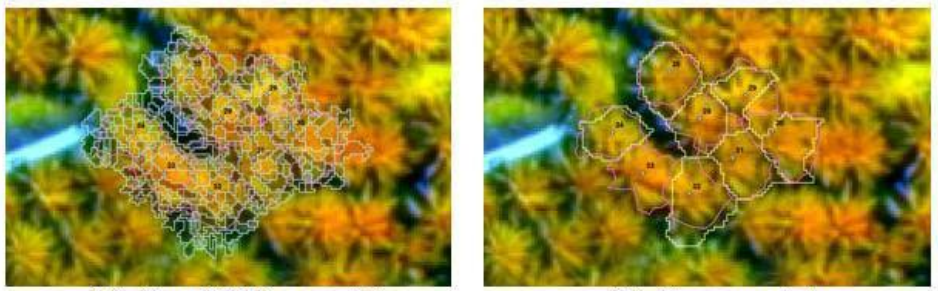

(a) Normal RGB segmentation (b) New segmentation

Figure 5: Segmentation results

5. DISCUSSIONS

The algorithm presented in this paper was indeed successful using three vegetation indices to improve segmentation of an individual oil palm trees. Amongst the vegetation indices that are used as pixel filter are the NDVI, NDII and DVI. Although not something new, the idea to reduce a multi-object into greyscale single-object level through a pixel filtering before performing the watershed segmentation, has shown good result where it can achieve up to 100% detection of total trees inside the plantation area. In fact, it was efficiently applied in some previous work where a homogeneous images were individually detected and segmented using watershed technique segmentation (Jing, Hu et al. 2012). Xia et al (2007) presented an image analysis where objects were efficiently segmented based on the point of viewing it's mean clustered spectral value, which having a similarities with our work but only the scope was more focused to a single-object greyscale layer. In parallel to that situation, we also implemented a strategic threshold parameter tuning where the solution was easily converged.

However, it is always difficult to get a perfect segment for the objects. The algorithm's challenge is to predict between the line of vegetation biomass level where other vegetations must be clearly differentiated from the oil palm biomass such as the grass and shrubs. Imperfections during filter phase often occurred during the pre-processing step where the isolated extreme value pixel inside object bodies was also filtered out. This event leaves a pixel's hole within the object bodies which was difficult to be segmented later and thus resulted in under segmentation cases. In contrast, over segmentation did also occur during the segmentation process where in some consideration needed a post-segmentation efforts (Freddrich and Feitosa 2008). Here, an evaluations up to certain extend might be involved in the post segmentation process which was a hanky-panky efforts. A simple algorithm without post-segmentation are preferred because it is easy, less complicated and also time efficient process which become a priority in this paper. What's next? As a recommendation, manual interruptions should be avoided in the middle

of the detection process which is going to be a smart and intelligent algorithm.

It is very important to get a reliable result out of the segmentation algorithm above. Outcome from the suggested segmentation algorithm in this paper has been proven as reliable and robust which produces a stable result although repeated many times with different threshold values. Although the success segmentation rate is good but it is not yet being tested on a various age stages of the oil palm. For the time being we are restricted to test the algorithm only on old palm plantation area which in the future we may further extend our research unto a younger oil palm. The assessment method suggested in this study also depended too much on the human observation which may often be subjected to changes. Besides, it needs a red edge band which is usually not available in most high resolution satellite images such as SPOT, Ikonos, QuickBird and digital aerial photo. In terms of price, a Worldview02 image is normally a little bit expensive compare to the others in its class.

ACKNOWLEDGEMENT

Special and many thanks to FELCRA Sabah Sdn Bhd for giving us the approval to use their site for this research study. I would also like to express our gratitude and acknowledgement to FFPRI, Tsukuba for funding the images.

REFERENCES:

(FAO), F. a. A. O. o. t. U. N. (1970). The Oil Palm. Ivory Coast, AFRICA.
Addink, E. A., S. M. De Jong, S. A. Davis, V. Dubyanskiy, L. A. Burdelov and H. Leirs (2010). "The use of high-resolution remote sensing for plague surveillance in Kazakhstan." Remote Sensing of Environment **114**(3): 674-681.
Addink, E. A., F. M. B. Van Coillie and S. M. De Jong (2012). "Introduction to the GEOBIA 2010 special issue: From pixels to geographic objects in remote sensing image analysis." International Journal of Applied Earth Observation and Geoinformation **15**(0): 1-6.
Agüera, F. and J. G. Liu (2009). "Automatic greenhouse delineation from QuickBird and Ikonos satellite images." Computers and Electronics in Agriculture **66**(2): 191-200.
Akasheh, O. Z., C. M. U. Neale and H. Jayanthi (2008). "Detailed mapping of riparian vegetation in the middle Rio Grande River using high resolution multi-spectral airborne remote sensing." Journal of Arid Environments **72**(9): 1734-1744.
Akbari, H., L. Shea Rose and H. Taha (2003). "Analyzing the land cover of an urban environment using high-resolution orthophotos." Landscape and Urban Planning **63**(1): 1-14.
Aksoy, B. and M. Ercanoglu (2012). "Landslide identification and classification by object-based image analysis and fuzzy logic: An example from the Azdavay region (Kastamonu, Turkey)." Computers & Geosciences **38**(1): 87-98.
Anagnostou, M. N., J. Kalogiros, E. N. Anagnostou, M. Tarolli, A. Papadopoulos and M. Borga (2010). "Performance evaluation of high-resolution rainfall estimation by X-band dual-polarization radar for flash flood applications in mountainous basins." Journal of Hydrology **394**(1–2): 4-16.
Ardila, J. P., V. A. Tolpekin, W. Bijker and A. Stein (2011). "Markov-random-field-based super-resolution mapping for identification of urban trees in VHR images." ISPRS Journal of Photogrammetry and Remote Sensing **66**(6): 762-775.
Blaschke, T. (2010). "Object based image analysis for remote sensing." ISPRS Journal of Photogrammetry and Remote Sensing **65**(1): 2-16.
Bunting, P., W. He, R. Zwiggelaar, R. Lucas, S. Jones and K. Reinke (2009). Combining Texture and Hyperspectral Information for the Classification of Tree Species in Australian Savanna Woodlands
Innovations in Remote Sensing and Photogrammetry. W. Cartwright, G. Gartner, L. Meng and M. P. Peterson, Springer Berlin Heidelberg**:** 19-26.
Chang, A., Y. Eo, S. Kim, Y. Kim and Y. Kim (2011). "Canopy-cover thematic-map generation for Military Map products using remote sensing data in inaccessible areas." Landscape and Ecological Engineering **7**(2): 263-274.
Clinton, N., A. Holt, J. Scarborough, L. Yan and P. Gong (2010). "Accuracy Assessment Measures for Object-based Image Segmentation Goodness." Photogrammetric Engineering and Remote Sensing **76**(3): 289-299.
Foody, G. M., D. S. Boyd and M. E. J. Cutler (2003). "Predictive relations of tropical forest biomass from

Landsat TM data and their transferability between regions." Remote Sensing of Environment **85**(4): 463-474.
Fornes, A., G. Basterretxea, A. Orfila, A. Jordi, A. Alvarez and J. Tintore (2006). "Mapping Posidonia oceanica from IKONOS." ISPRS Journal of Photogrammetry and Remote Sensing **60**(5): 315-322.
Freddrich, C. M. B. and R. Q. Feitosa (2008). Automatic Adaptation of Segmentation Parameters Applied to Non-Homogeneous Object Detection, Calgary, GEOBIA 2008 – Pixels, Objects, Intelligence: GEOgraphic Object-Based Image Analysis for the 21St Century.
Gonsamo, A. and P. Pellikka (2012). "The sensitivity based estimation of leaf area index from spectral vegetation indices." ISPRS Journal of Photogrammetry and Remote Sensing **70**(0): 15-25.
Hardisky, M. A., V. Klemas and R. M. Smart (1983). "The Influences of Soil Salinity, Growth Form, and Leaf Moisture on the Spectral Reflectance of *Spartina alterniflora* Canopies." Photogrammetric Engineering and Remote Sensing **49**(1): 77-83.
Hay, G. J. and T. Blaschke (2010). "Special Issue: Geographic Object-Based Image Analysis (GEOBIA) Foreword." Photogrammetric Engineering and Remote Sensing **76**(2): 121-122.
Hu, L., Z. Gong, J. Li and J. Zhu (2009). "Estimation of canopy gap size and gap shape using a hemispherical photograph." Trees - Structure and Function **23**(5): 1101-1108.
Jing, L., B. Hu, T. Noland and J. Li (2012). "An individual tree crown delineation method based on multi-scale segmentation of imagery." ISPRS Journal of Photogrammetry and Remote Sensing **70**(0): 88-98.
Korom, A. and M.-H. Phua (2011). Object-based Extraction of Individual Oil Palm Trees from GeoEye Satellite Image. 10th International Symposium & Exhibition of Geoinformation (ISG2011) and ISPRS Commission II/5 & II/7, Shah Alam, Selangor, MALAYSIA.
Koukoulas, S. and G. A. Blackburn (2005). "Mapping individual tree location, height and species in broadleaved deciduous forest using airborne LIDAR and multi-spectral remotely sensed data." International Journal of Remote Sensing **26**(3): 431-455.
Krause, G., M. Bock, U. Saint-Paul and H. Schneider (2010). Synoptic Analysis of Mangroves for Coastal Zone Management
Mangrove Dynamics and Management in North Brazil, Springer Berlin Heidelberg. **211:** 153-167.
Kwak, D. A., W. K. Lee, J. H. Lee, G. S. Biging and P. Gong (2007). "Detection of individual trees and estimation of tree height using LiDAR data." Journal of Forest Research **12**(6): 425-434.
Leckie, D. G., F. A. Gougeon, S. Tinis, T. Nelson, C. N. Burnett and D. Paradine (2005). "Automated tree recognition in old growth conifer stands with high resolution digital imagery." Remote Sensing of Environment **94**(3): 311-326.
Morel, A. C., J. B. Fisher and Y. Malhi (2012). "Evaluating the potential to monitor aboveground biomass in forest and oil palm in Sabah, Malaysia, for 2000–2008 with Landsat ETM+ and ALOS-PALSAR." International Journal of Remote Sensing **33**(11): 3614-3639.
Morel, A. C., S. S. Saatchi, Y. Malhi, N. J. Berry, L. Banin, D. Burslem, R. Nilus and R. C. Ong (2011). "Estimating aboveground biomass in forest and oil palm plantation in Sabah, Malaysian Borneo using ALOS PALSAR data." Forest Ecology and Management **262**(9): 1786-1798.
Möller, M., L. Lymburner and M. Volk (2007). "The comparison index: A tool for assessing the accuracy of image segmentation." International Journal of Applied Earth Observation and Geoinformation **9**(3): 311-321.
Peña-Barragán, J. M., M. K. Ngugi, R. E. Plant and J. Six (2011). "Object-based crop identification using multiple vegetation indices, textural features and crop phenology." Remote Sensing of Environment **115**(6): 1301-1316.
Richardson, A. J. and J. H. Everitt (1992). "Using spectral vegetation indices to estimate rangeland productivity." Geocarto International **7**(1): 63-69.
Rouse, J. W., R. H. Haas, J. A. Schell and D. W. Deering (1974). Monitoring Vegetation Systems in the Great Plains with ERTS. Third Earth Resources Technology Satellite-1 ERTS Symposium, NASA SP-351.
Santoso, H., T. Gunawan, R. Jatmiko, W. Darmosarkoro and B. Minasny (2011). "Mapping and identifying basal stem rot disease in oil palms in North Sumatra with QuickBird imagery." Precision Agriculture **12**(2): 233-248.
Tansey, K., I. Chambers, A. Anstee, A. Denniss and A. Lamb (2009). "Object-oriented classification of very high resolution airborne imagery for the extraction of hedgerows and field margin cover in agricultural areas." Applied Geography **29**(2): 145-157.
Thenkabail, P. S., N. Stucky, B. W. Griscom, M. S. Ashton, J. Diels, B. Van der Meer and E. Enclona (2004). "Biomass estimations and carbon stock calculations in the oil palm plantations of African derived

savannas using IKONOS data." International Journal of Remote Sensing **25**(23): 5447-5472.
Wang, L., A. Birt, C. Lafon, D. Cairns, R. Coulson, M. Tchakerian, W. Xi, S. Popescu and J. Guldin (2011). "Computer-based synthetic data to assess the tree delineation algorithm from airborne LiDAR survey." GeoInformatica: 1-27.
Wulder, M., K. O. Niemann and D. G. Goodenough (2000). "Local Maximum Filtering for the Extraction of Tree Locations and Basal Area from High Spatial Resolution Imagery." Remote Sensing of Environment **73**(1): 103-114.
Xia, Y., D. Feng, T. Wang, R. Zhao and Y. Zhang (2007). "Image segmentation by clustering of spatial patterns." Pattern Recognition Letters **28**(12): 1548-1555.
Zhang, K. Q. (2008). "Identification of gaps in mangrove forests with airborne LIDAR." Remote Sensing of Environment **112**(5): 2309-2325.